The catalytic behaviour of different sizes of dendrimer encapsulated Au_n nanoparticles in the oxidative degradation of morin with H_2O_2

Mulisa Nemanashi[a], Reinout Meijboom*[a]

[a] *Department of Chemistry, University of Johannesburg, P.O. Box 524, South Africa, Johannesburg, Auckland park 2006*. South Africa

Tel: +27(0)11 5592367, Fax: +27(0)11 5592816, E-mail: rmeijboom@uj.ac.za

Supplementary information

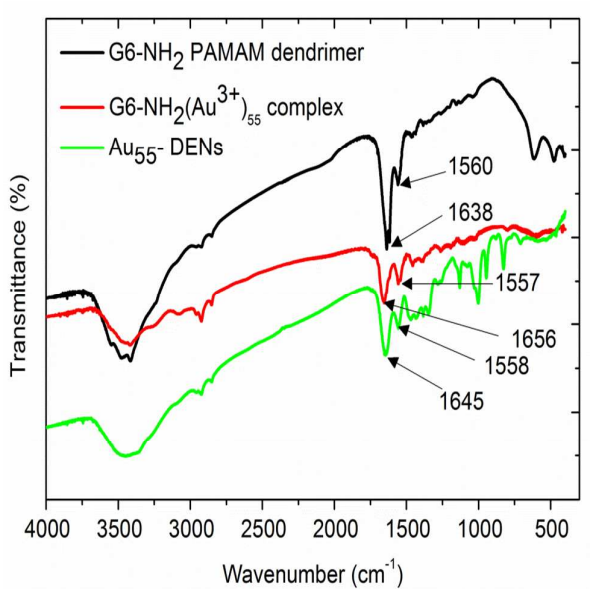

Figure S1: FTIR spectra of G6-NH_2 PAMAM dendrimer (80 µM), G6-$NH_2(Au^{3+})_{55}$ complex and Au_{55}-DENs.

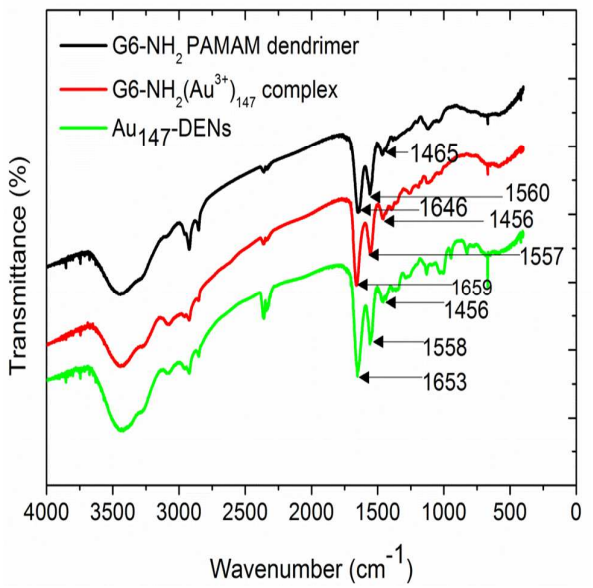

Figure S2: FTIR spectra of G6-NH_2 PAMAM dendrimer (80 µM), G6-$NH_2(Au^{3+})_{147}$ complex and Au_{147}-DENs.

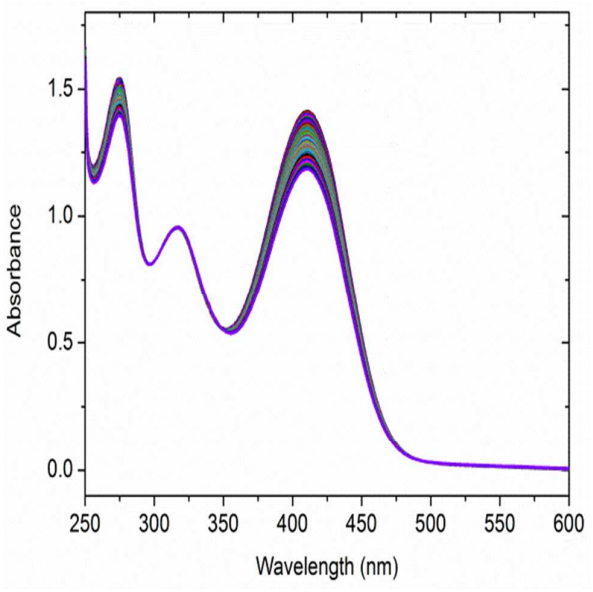

Figure S3: Time-based UV-vis spectra of morin solution (0.1 mM) with H_2O_2 (10 mM) in a carbonate buffer solution (50 mM) at pH 10 and 298 K for the catalytic oxidation of morin in the absence of a catalyst (spectrum taken every 10 minutes).

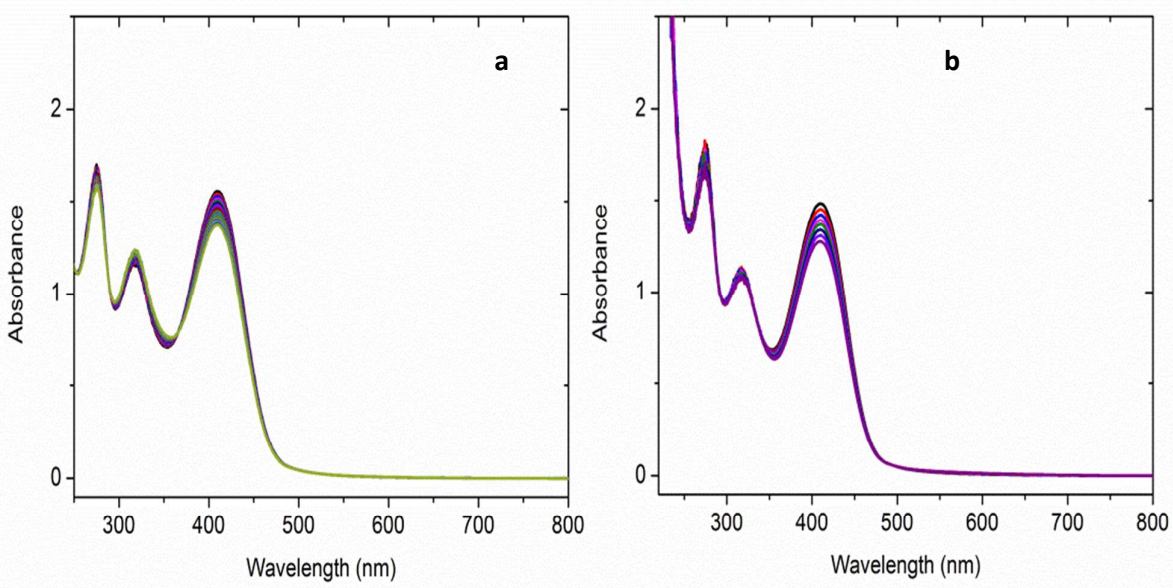

Figure S4: Oxidation of morin with H_2O_2 in the presence of a) aqueous dendrimer solution and b) the presence of Au-dendrimer complex. [morin]: 0.1 mM, Each spectrum was taken after 10 minutes.

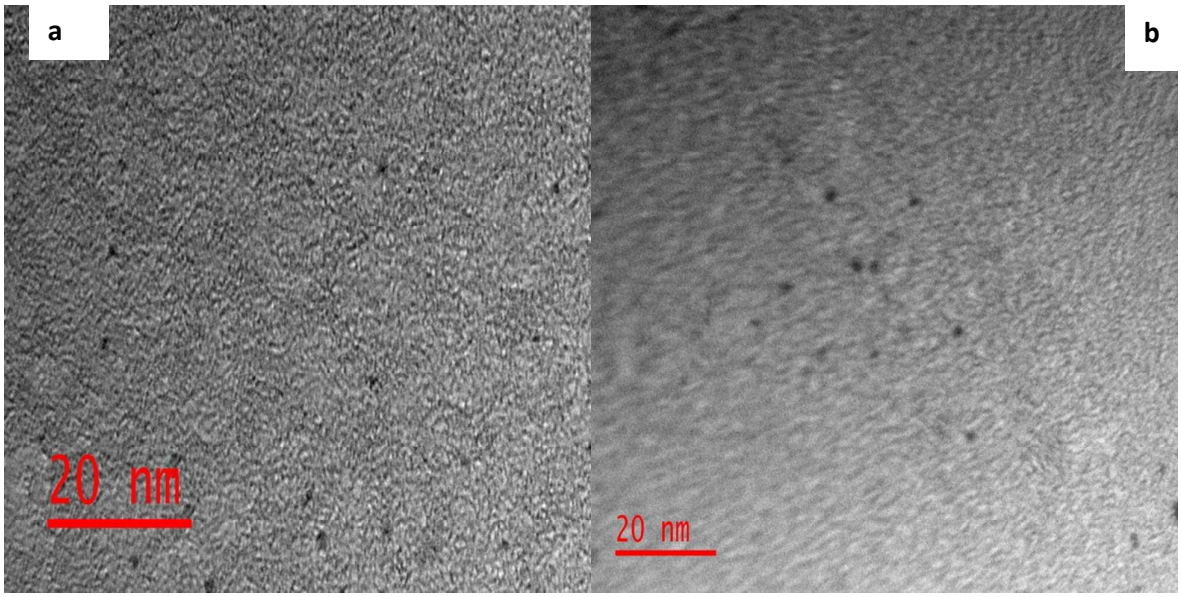

Figure S5: HRTEM images of the reaction products for the catalyzed oxidation of morin by H_2O_2 a) Au_{55}-DENs and b) Au-$_{147}$-DENs

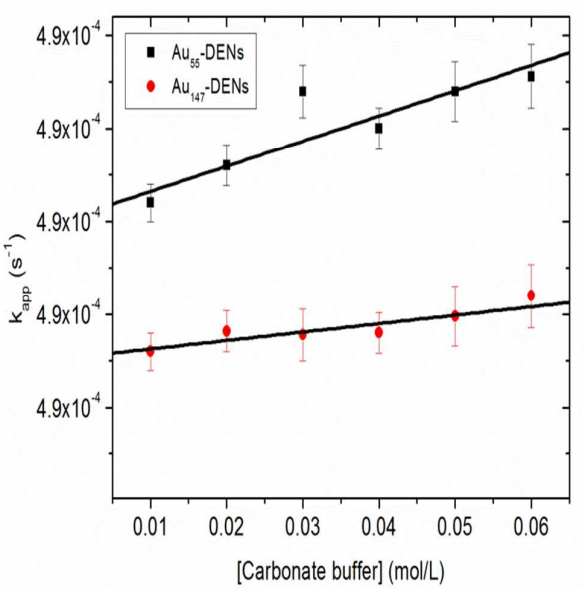

Figure S6: The effect of carbonate concentration in the apparent rate constant, k_{app}, during morin oxidation in the presence of H_2O_2 and Au_{55}- and Au_{147}-DENs catalyst. [morin]: 0.15 mM, [H_20_2]: 5 mM, [Au_{55}-DENs]: 0.81 m^2/L, [Au_{147}-DENs]: 0.91 m^2/L

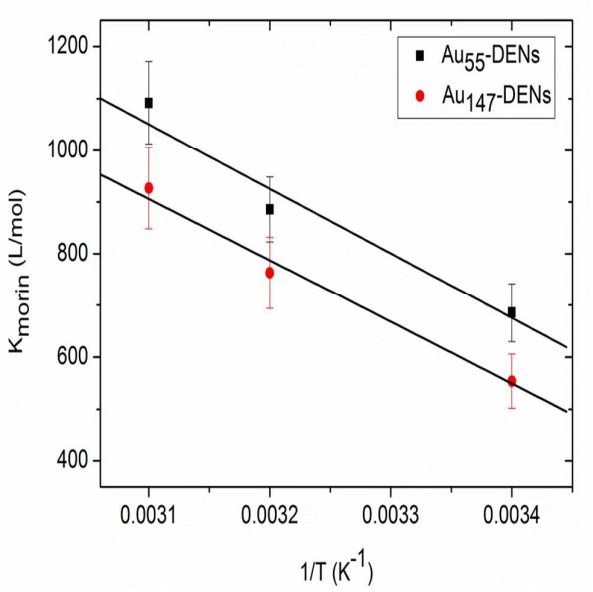

Figure S7: Plots for illustration of the dependency of adsorption constant of morin on temperature for Au_{55}-DENs and Au_{147}-DENs catalyst.

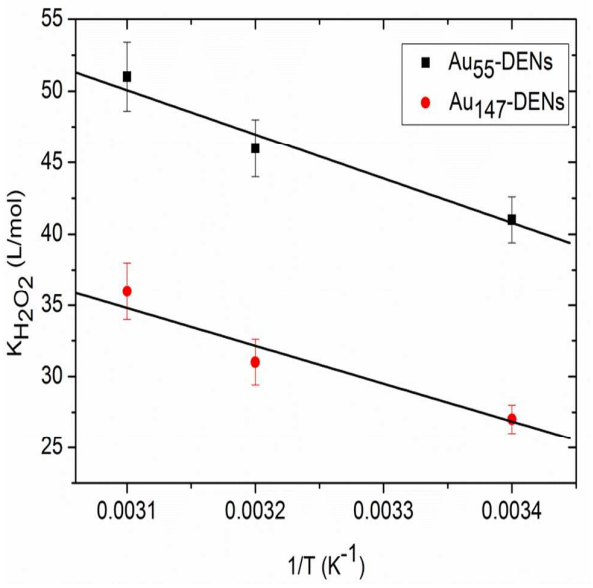

Figure S8: Plots for illustration of the dependency of adsorption constant of H_2O_2 on temperature for Au_{55}-DENs and Au_{147}-DENs catalyst.

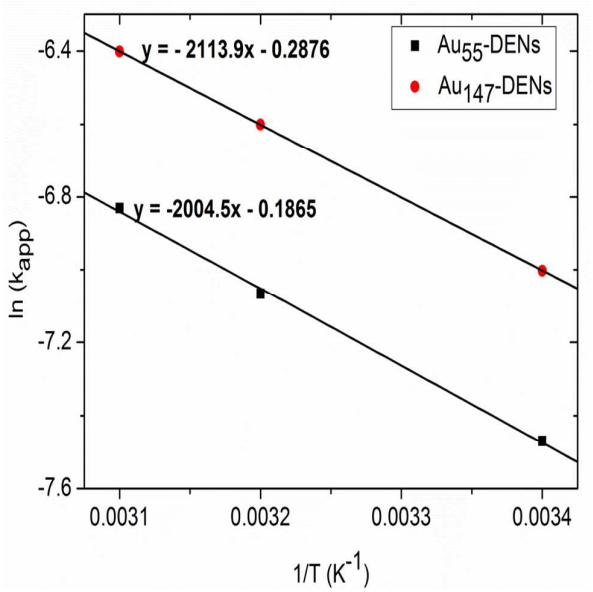

Figure S9: Arrhenius plots from which activation energies for k_{app} for Au_{55}-DENs and Au_{147}-DENs catalysts were calculated from.

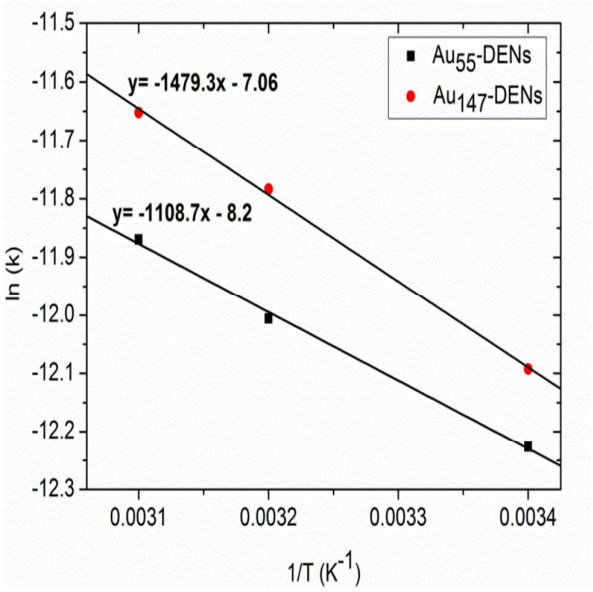

Figure S10: Arrhenius plots from which activation energies for surface rate, k, were calculated for both Au_{55}-DENs and Au_{147}-DENs catalysts.

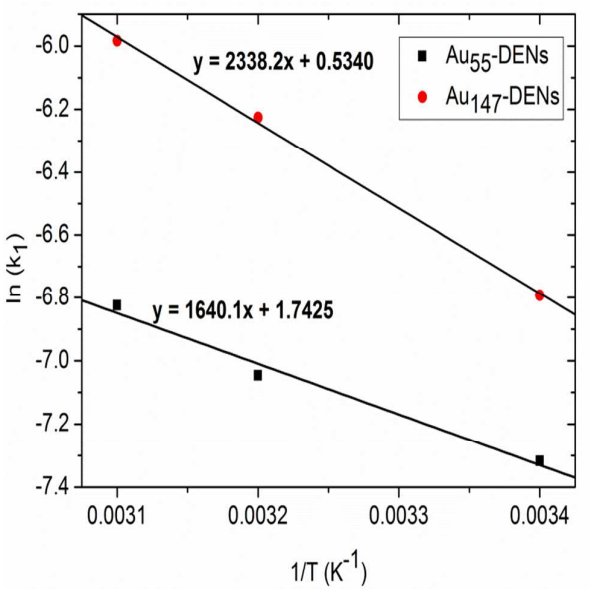

Figure S11: Arrhenius plots and equations from which activation energies for normalized rate constant, $k_{1,}$ were calculated for both Au_{55}-DENs and Au_{147}-DENs catalysts.

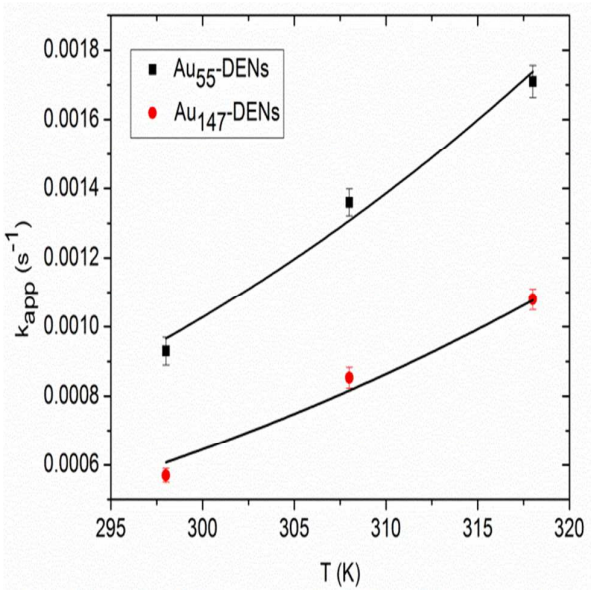

Figure S12: Eyring plots from which $\Delta H^{\ddagger}$, $\Delta S^{\ddagger}$, $\Delta G^{\ddagger}$ for k_{app} were calculated from.

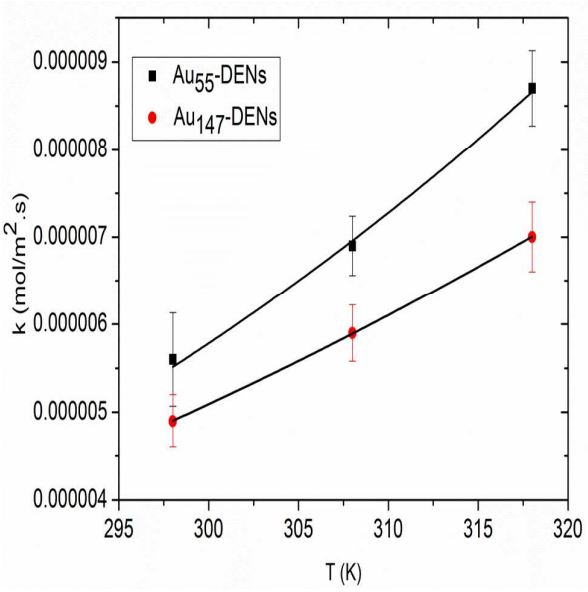

Figure S13: Eyring plots from which $\Delta H^{\ddagger}$, $\Delta S^{\ddagger}$, $\Delta G^{\ddagger}$ for surface rate, k, were calculated from.

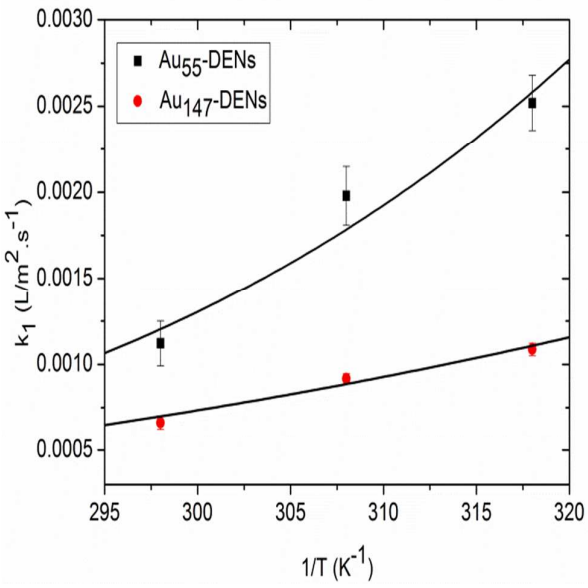

Figure S14: Eyring plots from which $\Delta H^{\ddagger}$, $\Delta S^{\ddagger}$, $\Delta G^{\ddagger}$ for normalized reaction rate, k_1, were calculated from.

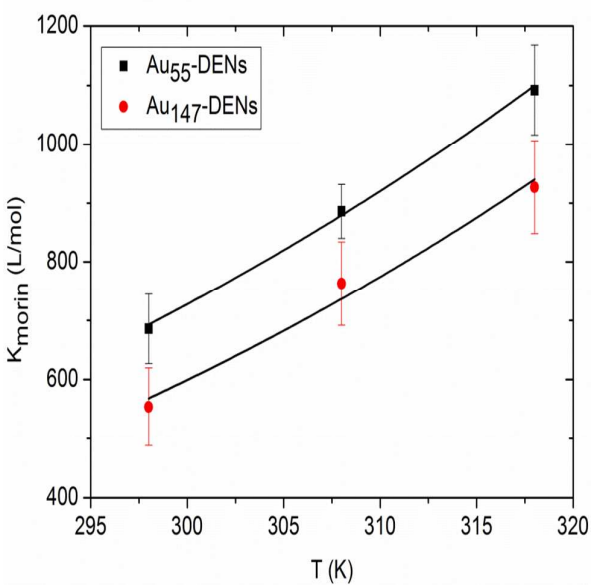

Figure S15: Eyring plots from which $\Delta H^{\ddagger}$, $\Delta S^{\ddagger}$, $\Delta G^{\ddagger}$ for adsorption constant of morin, K_{morin} , were calculated from.

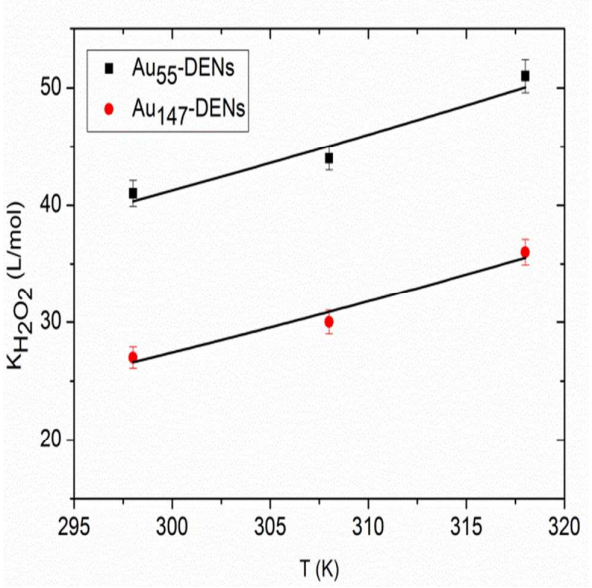

Figure S16: Eyring plots from which $\Delta H^{\ddagger}$, $\Delta S^{\ddagger}$, $\Delta G^{\ddagger}$ for adsorption constant of H_2O_2, $K_{H_2O_2}$, were calculated from.